TIANJIN SUBURBS PS-QPS ANALYSIS AND VALIDATION WITH LEVELING DATA

Qingli Luo[1], Daniele Perissin[1], Ozan Dogan[1], Hui Lin[1], Wei Wang[2]*

[1]Institute of Space and Earth Information Science, The Chinese University of Hong Kong, Hong Kong SAR, China

[2]Tianjin Institute of Surveying and Mapping, Tianjin, China

* Corresponding author, email: daniele.perissin@cuhk.edu.hk

ABSTRACT

Permanent Scatterers (PS) based on Synthetic Aperture Radar (SAR) data has been approved to be a feasible way to detect and monitor wide area ground subsidence at a low cost. Classical PS algorithms are focused on exploring the point-like radar targets while Quasi-PS (QPS) technique was proposed to manage the detection of both distributed and decorrelating targets. In this work, we explore the potential ability of PS and QPS analysis for subsidence monitoring with L- and X-band. A case study was conducted in Tianjin suburbs and the exploited SAR datasets were composed of 23 ALOS images acquired from 2009/4/24 to 2010/10/28 and 37 TerraSAR-X images from 2009/4/29 to 2010/11/11. The average subsidence velocity map and displacement history have been retrieved by PS and QPS analysis and the validation indicates good agreement between INSAR time series results and leveling data.

Index Terms— Permanent Scatterers (PS); Quasi-PS (QPS); Tianjin; validation

1. INTRODUCTION

Urban development and overexploitation of groundwater make Tianjin to be one of the major subsidence regions of China. In recent years, subsidence rate in downtown area of Tianjin tend to slow down with the control of strict rules. However, with the development of rural economy and lack of supervision, several new subsidence centers occurred in the suburbs and the subsidence rate is even higher than the old ones. More attention is required on suburbs. Differential Interferometric Synthetic Aperture Radar, (DINSAR), was approved to be a feasible way for wide area subsidence monitoring instead of the traditional leveling and GPS methods [1, 2]. However, DINSAR method is known to have two major limitations named as spatiotemporal decorrelation and atmospheric disturbance [3, 4]. In order to overcome these limitations, Permanent Scatterers (PS) [5, 6] was proposed as the first one of the Persistent Scatterers Interferometry [7-12] techniques and it has been proved to be 1 mm accuracy for deformation monitoring [13].

Classical PS algorithms that focus on exploring the point-like radar targets cannot achieve sufficient performance in extra-urban areas due to the low PS density. In order to extract information from partially coherent targets and thus to increase the spatial distribution of measured points, Quasi-PS (QPS) technique combined the analysis of phase spatial and temporal correlation. This method manages the detection of both distributed and decorrelating targets [14]. Compared with the classical PS technique, there are 3 main differences: 1) More than one reference images can be selected. 2) Partially coherent targets that are only coherent for a subset of interferograms can be monitored. 3) Spatial filtering can be applied. Via these modifications, distributed and decorrelating targets can be detected with the disadvantage of losing the accuracy and resolution. Several successful applications [14-15] confirm QPS and PS technique can be considered as complementary methods and they can be employed alternatively according to real constraints and requirements [14] in order to take the advantage of both methods. Exploring the monitoring ability of PS and QPS is useful for further applications of these two methodologies.

In this paper, taking Tianjin suburbs as the study area, we have carried out TSX PS analysis and ALOS QPS analysis for subsidence monitoring. The average velocity maps of TSX PS and ALOS QPS analyses have been carried out and the results validated with the leveling data.

2. STUDY AREA AND METHODOLOGY

Tianjin is located in the northeast of North China Plain and covers an area between 38 ° 34 ' and 40 ° 15'N, and between 116 ° 43 ' and 118 ° 04 'E. The case study area is located in the west of Tianjin downtown, including Wuqing district, Beichen district, Xiqing district and Jinghai County and several towns. SAR datasets are composed of 23 ALOS L-band images acquired between 2007/01/17 and 2010/10/28 and 37 TSX X-band images acquired between 2009/4/29 and 2010/11/11. In Figure 1, the spatial coverage of L-Band

(red rectangle) data and X-Band (blue one) data are presented overlaid with Google Earth (GE) map. ALOS (wavelength of 23cm) provides a wide coverage of 64 by 66 km (17082 pixels range direction by 20957 pixels azimuth direction), having a spatial resolution of approximately 7 m on the ground, with an incidence angle of about 38.70 degrees, along an ascending orbit (from South to North). TSX data has a better spatial resolution of approximately 3 m, with a coverage of 30 by 60 km (29636 pixels range direction by 31457 pixels azimuth direction), along descending orbit (from North to South), and the incidence angle is 41.08 degrees.

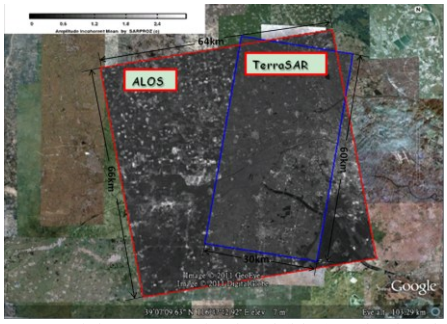

Figure 1. Spatial coverage of X-band (blue) and L-band (red).

Classical PS approach was applied to process the available TSX dataset while QPS analysis was used to process the ALOS dataset. In Figure 2, the two dataset parameters including the acquisition dates of reference and slave images, perpendicular baselines and time intervals are shown. Figure 2 (a) demonstrates all images of TSX dataset with reference to a master image which is acquired on November 13th, 2009. It should be noted that perpendicular baselines of all pairs are less than 200 m. The maximum normal and temporal baselines are 181m and 363 days, while the minimum ones are 1m and 11 days, respectively. For processing ALOS dataset, multiple reference images were selected and 98 interferograms generated as illustrated in Figure 2 (b) with the average coherence threshold of 0.25. The perpendicular baselines of ALOS interferometric pairs, no more than 4000m in this case, are far larger than that of TSX data because the longer wavelength of L-band allows better coherence even with large spatial baselines.

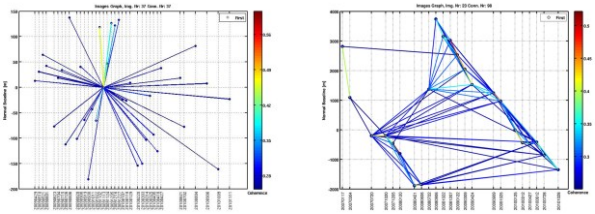

(a) TSX PS analysis (b) ALOS QPS analysis

Figure 2. Images graph. X-axis: temporal baseline of the acquisitions. Y-axis: normal baseline of the acquisitions. Color scale: average spatial coherence of the corresponding interferometric link.

The PS and QPS analysis are applied by the software SARPROZ [16], which provides data processing, data analysis, data visualization and data exportation in different formats. DEM from Shuttle Radar Topography Mission (SRTM) with 3 arcsec resolution was applied for topographic phase removal. There are two major outputs for each PS: average velocity map derived for the whole time period and displacement history [6], displayed exploiting GE imagery.

3. RESULTS AND ANALYSES

With the PS and QPS processing described in section 2, the average velocity map of X-band PS results and L-band QPS results are presented in Figure 3. More than 940,000 PS points (approximately 522 /km^2 with the temporal coherence threshold of 0.7) were identified by the PS analysis as illustrated in Figure 3 (a). However, the spatial distribution of these points is not homogeneous. Due to the location of the man-made objects, PS density varies from up to 0-10 /km^2 in the agricultural parcels to over 1500-2000 /km^2 in residential areas. Therefore, significant spatial gaps exist although there is large number of PS points. Figure 3 (a) shows that the velocity ranges from -60 to 20 mm/yr, which indicates a maximum subsidence rate of -80 mm/yr. The subsidence rate of red area is higher and the blue area is lower w.r.t a reference point. Three prime subsiding centers are detected in this area: Shengfang, Wangqingtuo and Nanhe Town. The subsidence rate of Wuqing and Jinghai district tends to slow down and more stable than before [17]. Nanhe Town is a newfound subsiding center without released subsidence information and more attention is required on that area.

Simultaneously, more than 3,867,649 QPS points (approximately 915/km^2 with the temporal coherence threshold of .7) were identified by QPS analysis as represented in Figure 3 (b). It seems that there are more QPS points than PS points per square kilometers. However, it can be noted that most of the PS points are identified as man-made objects and they are aggregated in residential areas, where the density of PS points is far more than that of QPS points. Unlike PS results, the spatial distribution of QPS points is homogeneous both for the agricultural parcels and residential areas. The reasonable explanation should be the longer wavelength of L-band supports good coherence even over the vegetation area, where more distributed targets exist instead of point-like targets and they can be detected by QPS analysis. Figure 3 (b) demonstrates the velocity ranging from -150 to 40 mm/yr, which shows the blue area lifted and the red area subsiding w.r.t a reference point. Similarly to PS results, the subsiding centers of Wangqingtuo, Shengfang and Nanhei Town can be also detected by QPS analysis. Although the coverage, colorbar, incidence angle, time span and reference point of these two average velocity maps are

different, the accordant subsidence tendency has been detected by both methodologies when applied to different band datasets. In order to validate the results of these two methodologies, quantitative comparison will be carried out in the next section.

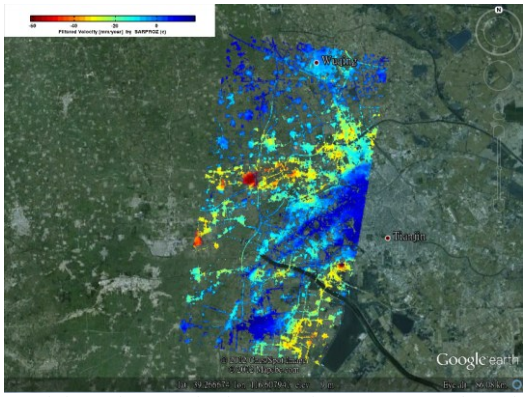

(a) Linear deformation trend of TSX using PSInSAR. The color scale shows stable areas in blue and moving areas in yellow (-30mm/yr) and red (-60mm/yr).

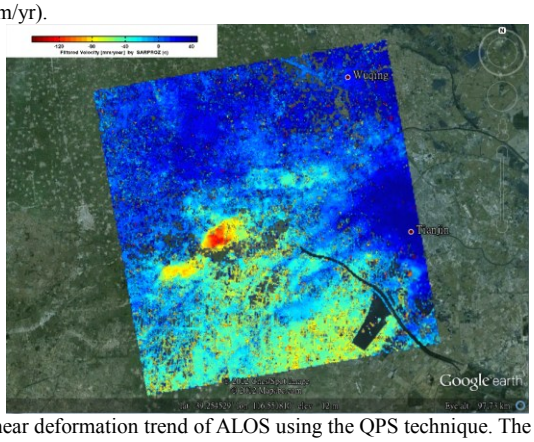

(b) Linear deformation trend of ALOS using the QPS technique. The color scale shows stable areas in blue and moving areas in yellow (-80mm/yr) and red (-150mm/yr).

Figure 3. Linear deformation trend along Line of Sight (LOS) direction.

4. VALIDATION WITH LEVELING

8 leveling points were provided for PS and QPS results validation. The elevations of these points were acquired at different time nodes by the method of national second-order leveling and the root-mean-square error is 2 mm/km for each leveling line. The height difference on those benchmarks between October 2009 and October 2010 are provided for validation, which has the accuracy of about 2.8 mm/km according to law of error propagation.

Before the comparison between leveling value and PS results, the possible sources of uncertainties include the following six parts. (1) The reference points between PS and leveling measurements in the time domain are missing. The leveling points were measured in October, 2009 and 2010 without exact acquisition date, resulting in one month uncertainty for these two time nodes. (2) The location of leveling point has an accuracy of 15m. (3) The reference PS point is assumed to be stable. However, it is not always true due to the subsiding throughout the whole area of Tianjin site. In addition, the "double difference" measurement of PS techniques increases this uncertain component. (4) PS is sensitive along LOS direction compared with the vertical of leveling. (5) Only few leveling data are provided and thus it probably introduces the gross errors during the comparison of the two distinct measurements. (6) The accuracy of the leveling reference point has been reduced because of the severe subsidence of Tianjin area.

Table 1. Displacement comparison between PS and leveling (mm)

ID	Leveling	PS	Error	RMSE
1	3.96	0.38	-3.57	6.21
2	-10.36	-9.45	0.92	
3	-24.69	-20.48	4.20	
4	-5.84	-10.56	-4.72	
5	3.96	12.97	9.01	
6	21.29	24.95	3.65	
7	20.54	23.39	2.85	
8	-8.86	-21.19	-12.33	

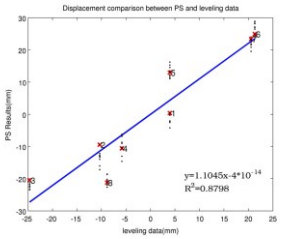

Figure 4. Displacement comparison of PS and leveling data

Leveling data were acquired in October each year without exact acquisition dates, and the height difference of two measurements are taken as the displacement. To validate PS results, the images acquired on 11th, October, 2009 and 9th, October, 2010 are selected as two time nodes for PS results. The nearest PS points are selected and the displacement between these two time nodes is calculated. In the following, quantitative displacement comparison between PS results and leveling data is illustrated in Table 1. The entire Root Mean Square Error (RMSE) is 6.21 mm, the minimum error is 0.92 mm and maximum is -12.33 mm. However, note that the subsidence rate of this area is fast, ranging from -60 to 20 mm/yr. Our estimation is the error for the whole year subsidence. If we convert it into days, the error is less than 0.02mm/day. The accuracy could be acceptable, considering fast subsidence over a large scale. In Figure 4, the linear regression is done between the nearest PS points highlighted with red dots and leveling points. The correlation coefficient is nearly 0.9, indicating good agreement between these two distinct measurements. Due to the uncertainties of the location of leveling points, to every leveling point, ten nearest PS points are selected and highlighted with black dots, whose distribution demonstrates the more authentic situation may be better or even worse than our estimation. Simultaneously, the average velocity of QPS analysis has been validated with the leveling data. The subsidence rate of QPS results is computed by the average of more than three years. However, subsidence observation over one year is assumed to be subsidence rate of leveling, which will increase uncertainty in the process of validation. The comparison listed in Table 2 presents the whole RMSE is 10.93 mm/yr, the maximum error is 21.75 mm/yr and the minimum is -2.05 mm/yr. In view of the whole region fast subsiding with range of -150 mm/yr to 40 mm/yr, the

relative error is 0.05, achieving the same accuracy as the published mm accuracy in case of mm subsidence [13]. Similarly, the linear regression between the QPS points highlighted with red dots and leveling points has been done. The correlation coefficient of nearly 0.7 suggests the results of QPS analysis is in accordance with leveling measurement.

Table 2. Average velocity comparison between QPS and leveling (mm/yr)

ID	Leveling	QPS	Error	RMSE
1	-34.34	-26.21	-8.13	10.93
2	-49.17	-35.11	-14.06	
3	-64.00	-72.22	8.22	
4	-44.48	-42.41	-2.07	
5	-34.34	-56.09	21.75	
6	-16.39	-6.32	-10.07	
7	-17.17	-23.60	6.43	
8	-47.61	-45.56	-2.05	

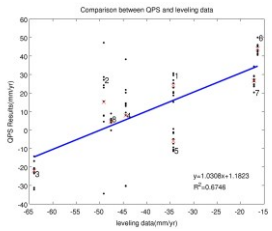

Figure 5. Average velocity comparison of QPS and leveling data

5. CONCLUSION

In this paper, we report the INSAR time series analysis results for subsidence monitoring in Tianjin suburbs, where we experimented PS and QPS analysis with X- and L-band, respectively. Three areas with obvious motion are detected from X-band PS and L-band QPS analysis, containing one newfound subsiding center. There are significant differences in the distribution of PS points between X-band PS and L-band QPS analysis results. The vast majority of PS points concentrated in residential areas and almost no PS points in residential areas from X-band PS results, due to the location of man-made objects. Comparatively, the spatial distribution of QPS points is more homogeneous, because longer wavelength of L-band allows good coherence even over vegetation areas and QPS technique detects distributed targets. The subsidence patterns derived from L- and X-band INSAR time series analysis are observed to have a good agreement, although they are acquired in different incidence angles and time periods with different wavelengths. The X-band PS quantitative analysis with the leveling data shows 0.9 correlation and 6 mm dispersion, indicating very good agreement even under the given ambiguities. Simultaneously, the average velocity validation of L-band QPS results achieves 0.7 correlation and 11 mm/yr dispersion, fitting well with leveling data under the condition of wide area fast subsiding.

6. ACKNOWLEDGMENT

TerraSAR-X data used in this work are provided by Infoterra. The software we used in this work is SARProz, developed by Daniele Perissin. This work was partially supported by the Research Grants Council (RGC) General Research Fund (GRF) (Proj. Ref. No.415911) of HKSAR. The authors were thankful to data and technical supports from Ke Hu, a chief engineer in Tianjin Institute of Surveying and Mapping.

7. REFERENCES

[1] Raucoules, D., C. Colesanti, and C. Carnec, *Use of SAR interferometry for detecting and assessing ground subsidence*. Comptes Rendus Geoscience, 2007. 339(5): p. 289-302.

[2] Rott, H., *Advances in interferometric synthetic aperture radar (InSAR) in earth system science*. Progress in Physical Geography, 2009. 33(6): p. 769-791.

[3] Zebker, H.A. and J. Villasenor, *Decorrelation in interferometric radar echoes*. IEEE Transactions on Geoscience and Remote Sensing , 1992. 30(5): p. 950-959.

[4] Zebker, H.A. and P. Rosen, *Atmospheric artifacts in interferometric SAR surface deformation and topographic maps*. J. Geophys. Res. Solid Earth, 1997. 102(4): p. 7547–7563.

[5] Ferretti, A., C. Prati, and F. Rocca, *Nonlinear subsidence rate estimation using permanent scatterers in differential SAR interferometry.* IEEE Transactions on Geoscience and Remote Sensing, 2000. **38**(5): p. 2202-2212.

[6] Ferretti, A., C. Prati, and F. Rocca, *Permanent scatterers in SAR interferometry.* IEEE Transactions on Geoscience and Remote Sensing, 2001. **39**(1): p. 8-20.

[7] Mallorquí, J.J., et al. *Linear and non-linear long-term terrain deformation with DInSAR (CPT: Coherent Pixels Technique)*. 2003.

[8] Mora, O., J.J. Mallorqui, and A. Broquetas, *Linear and nonlinear terrain deformation maps from a reduced set of interferometric SAR images.* IEEE Transactions on Geoscience and Remote Sensing, 2003. 41(10): p. 2243-2253.

[9] Werner, C., et al. *Interferometric point target analysis for deformation mapping*. 2004. IEEE.

[10] Kampes, B.M. and N. Adam. *The STUN algorithm for persistent scatterer interferometry*. in *Fringe 2005 Workshop*. 2006. earth.esa.int.

[11] Hooper, A., et al., *A new method for measuring deformation on volcanoes and other natural terrains using InSAR persistent scatterers.* Geophysical Research Letters, 2004. 31(23).

[12] Berardino, P., et al., *A new algorithm for surface deformation monitoring based on small baseline differential SAR interferograms.* IEEE Transactions on Geoscience and Remote Sensing, 2002. 40(11): p. 2375-2383.

[13] Ferretti, A., et al., *Submillimeter accuracy of InSAR time series: Experimental validation.* IEEE Transactions on Geoscience and Remote Sensing, 2007. 45(5): p. 1142-1153.

[14] Perissin, D. and W. Teng, *Repeat-Pass SAR Interferometry With Partially Coherent Targets.* IEEE Transactions on Geoscience and Remote Sensing, 2012. 50(1): p. 271-280.

[15] Perissin, D. and T. Wang, *Time-Series InSAR Applications Over Urban Areas in China.* Ieee Journal of Selected Topics in Applied Earth Observations and Remote Sensing, 2011. 4(1): p. 92-100.

[16] Perissin, D., *SARPROZ software manual.* http://ihome.cuhk.edu.hk/~b122066/manual/index.html.

[17] Xie Dake, Wang Miao, and Xu Dong, *Researching on sub-regional management of land subsidence in Tianjin.* Modern Water, 2009. 4: p. 36-38.